UDC 621.921.34:661.65:537.31

D. Prikhodko[1, 2, *], S. Tarelkin[1, 3], V. Bormashov[1, 2, 4], A. Golovanov[1, 2], M. Kuznetsov[1], D. Teteruk[1], N. Kornilov[1], A. Volkov[1], A. Buga[1, 2]

[1]Technological Institute for Superhard and Novel Carbon Materials, Troitsk, Moscow, Russia

[2]Moscow Institute of Physics and Technology, Moscow Region, Russia

[3]National University of Science and Technology MISiS, Moscow, Russia

[4]The All-Russian Research Institute for Optical and Physical Measurements (VNIIOFI), Moscow, Russia

**dmprikhodko@gmail.com*

Low temperature thermal conductivity of heavily boron-doped synthetic diamond: Influence of boron-related structure defects

Thermal conductivity of single-crystal boron-doped diamonds (BDD) with ~ $2 \cdot 10^{19}$ cm^{-3} (~ 120 ppm) and $5 \cdot 10^{19}$ cm^{-3} (~ 300 ppm) boron content was studied by a steady-state method in a temperature range of 20–400. K. The obtained data were analyzed within Callaway model framework. The values of dislocation density obtained from best fit of experimental data and from density of etch pits measuring were compared. Their discrepancy suggests presence of some other boron-related defects in crystal lattice.

***Keywords**: boron-doped diamond; thermal conductivity; HPHT; dislocation density.*

INTRODUCTION

Diamond is known as the best thermal conductor. In [1–4] temperature dependencies of thermal conductivity of pure single crystal diamonds were measured and analyzed within the frameworks of Debye and Callaway models. The dominating role of phonon scattering on isotope ^{13}C atoms in thermal conductivity reduction has been deduced. Studies [1–4] showed that the thermal conductivity of diamond can be calculated using Callaway model [5] and the model parameters for normal and umklapp processes have been evaluated. However, the influence of different defects on thermal conductivity was not analyzed.

Boron-doped II*b*-type diamonds (BDD) are *p*-type semiconductors extensively used in design of high-power, high-frequency, high temperature electronic devices [6–8]. Thermal conductivity of single-crystal BDD is an important parameter for electronic devices but it is much less investigated comparing to undoped II*a*-type diamonds. Recently we studied experimentally thermal conductivity of samples cut from single-crystal BDD with ~ $5 \cdot 10^{18}$ cm^{-3} boron content and from pure II*a*-type diamond in the temperature range of 20–400 K [9]. We found that extended defects like dislocations have much stronger influence on thermal conductivity of BDD

than point defects. The parameters of Callaway model characterizing phonon scattering on dislocations were estimated.

In the present work we studied thermal conductivity of two samples cut from different single-crystal BDD with boron content higher than 10^{19} cm^{-3} in the same temperature range. It is known that diamonds with boron content higher than $\sim 4 \cdot 10^{18}$ cm^{-3} have octahedral habitus instead of cubooctahedral one [10]. The growth rate of (100) edge decreases substantially, thus the density of point and extended defects may increase in a different way. In [9] BDD sample had cubooctahedral habitus, while raw diamonds studied in this work have the octahedral one.

EXPERIMENTAL DESIGN

We employed Physical Properties Measurement System™ (PPMS) by Quantum Design with close cycle cryostat (EverCool-II) to achieve vacuum better than 10^{-5} Torr and high temperature accuracy and stability. The thermal conductivity measurements were carried out by the steady-state method. This method is widely used for thermal conductivity measurements. Its detailed description can be found elsewhere [9, 10]. The design of the diamond sample for thermal conductivity measurements is shown in Fig. 1.

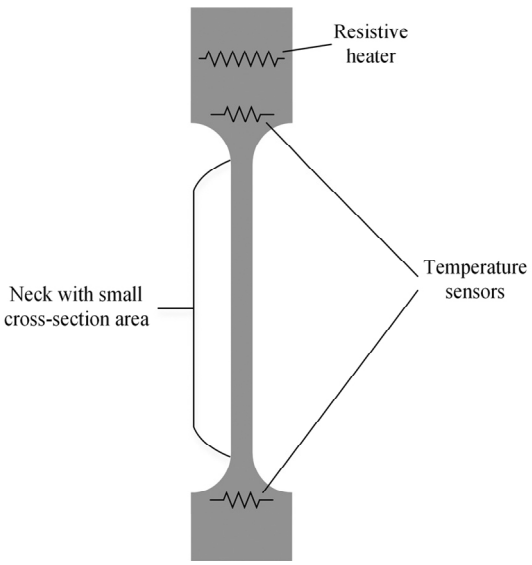

Fig. 1. Design of the diamond sample for the steady-state method.

SAMPLES PREPARATION

We investigated synthetic single-crystal diamonds grown by the temperature gradient method under high pressure and high temperature (HPHT) in a "toroid" type high-pressure apparatus. 1.52 and 3.61 at % of amorphous boron powder was added to the carbon source for II*b*-type diamond growth. The resulted boron content in the grown BDD crystals was ~ $2 \cdot 10^{19}$ cm^{-3} (~ 120 ppm) and $5 \cdot 10^{19}$ cm^{-3} (~ 300 ppm). BDD crystal with $5 \cdot 10^{19}$ cm^{-3} of boron is shown in Fig. 2, *b*. Diamond sample with $2 \cdot 10^{19}$ cm^{-3} boron had the same shape and color.

One can see that crystals in Figs. 2, *a* and 2, *b* have different habits. Such change of habits consistently takes place when boron content exceeds 10^{19} cm^{-3}. More details of the growth process, electrical properties and heat capacity of sin-

gle-crystal BDD were described in [11–13]. We used proprietary laser cut system to prepare (001) plates from grown crystals, and then mechanically polished them. The resulting thickness of plates was about 180 μm. X-ray topography images of fabricated plates are shown in Fig. 3.

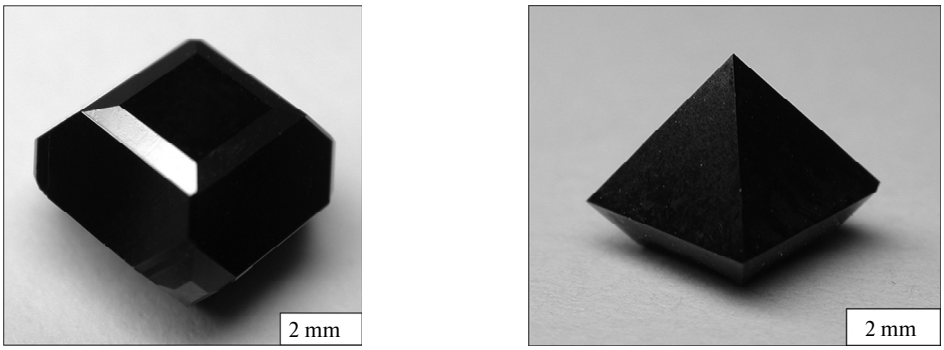

a *b*

Fig. 2. As-grown diamonds: ~ $5 \cdot 10^{18}$ (*a*) and ~ $5 \cdot 10^{19}$ (*b*) cm^{-3} of boron.

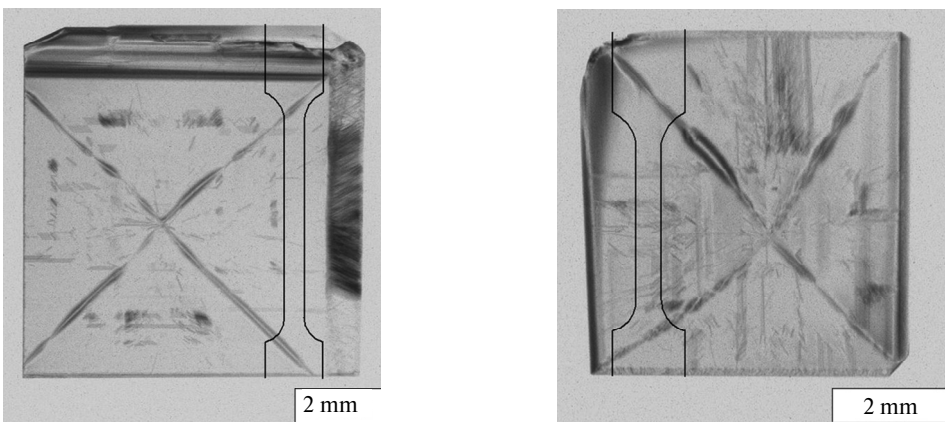

a *b*

Fig 3. X-ray diffraction topography of BDDs with $2 \cdot 10^{19}$ (*a*) and $5 \cdot 10^{19}$ (*b*) cm^{-3} of boron. Contours of samples for thermal conductivity measurements are pointed out.

To ensure the electrical isolation between metallic contacts used for temperature sensors and heater the thin (~ 10 μm) insulating layer of high pure diamond was grown homoepitaxially on each plate in microwave plasma reactor by PLASSYS. After proper treatment of the diamond plates surfaces three platinum resistors of ~ 1 kΩ resistance have been deposited using lift-off optical lithography and magnetron sputtering (Fig. 4). They act as a resistive heater and two temperature sensors for hot and cold sample edges.

Due to a very high thermal conductivity of diamond, we decided to decrease sample cross-section and, therefore, increase heat pulse propagation time for more reliable measurements. Thus, the sample geometry was modified by laser cutting to create a narrow neck of 0.3 mm width and 2.7 and 4 mm length (for 300 and 120 ppm samples respectively). Contours of the finally cut samples and their position with respect to the entire plates are shown in Fig. 3.

Commercial PPMS chuck was used for mounting of samples. It provides electrical connections of sensors and the heater and acts as a thermal bath. The

electrical leads were made using a conventional ultrasonic thermal-compression welding (Fig. 5).

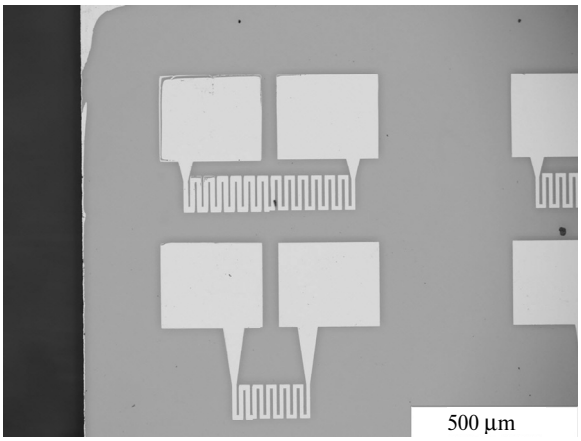

Fig. 4. Electrical heater (top) and resistive temperature sensor (bottom) at the upper end of the sample (before cut).

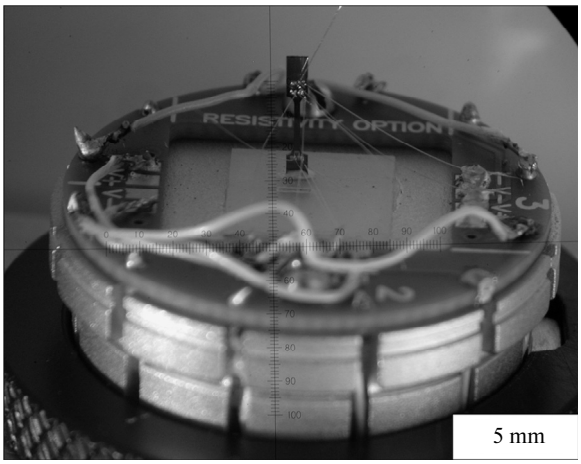

Fig. 5. BDD sample installed on the sample holder.

EXPERIMENTAL RESULTS AND DISCUSSION

Measurement results collected on both boron-doped diamond samples are presented in Fig. 7. The results for II*a* diamond and BDD with $5{\cdot}10^{18}$ cm^{-3} boron content from [9] are shown for comparison.

It is clearly seen that the thermal conductivity decreases with the boron content increase. At room temperature it drops from about 2300 W/(m·K) for II*a*-type diamond to about 500 W/(m·K) for BDD with $5{\cdot}10^{19}$ cm^{-3} boron content. Unlike II*a*-type diamond and BDD with ~ $5{\cdot}10^{18}$ cm^{-3} boron, the thermal conductivity of BDDs with $2{\cdot}10^{19}$ cm^{-3} and $5{\cdot}10^{19}$ cm^{-3} boron does not have evident maximum in a low temperature range. At ~ 100 K II*a*-type diamond has thermal conductivity of about 17000 W/(m·K), while sample with the highest boron content has thermal conductivity about 250 W/(m·K), that is about 70 times less.

Following the results of our previous work, we focused on dislocations density in new samples. We estimated the number of dislocations by counting the etch pits.

To count etch pits we etched properly polished and cleaned diamond surface in H_2/O_2 plasma for 10 minutes at ~ 850 °C. We also etched BDD plate with $5 \cdot 10^{18}$ cm^{-3} boron content to compare with more heavily doped crystals. The images of etched surfaces are shown in Fig. 6.

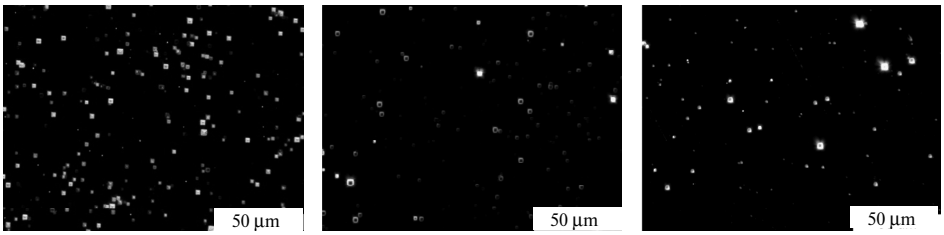

a *b* *c*

Fig. 6. Etched surfaces of diamonds with different boron content: ~ $5 \cdot 10^{18}$ (*a*), ~ $2 \cdot 10^{19}$ (*b*), ~ $5 \cdot 10^{19}$ (*c*) cm^{-3}.

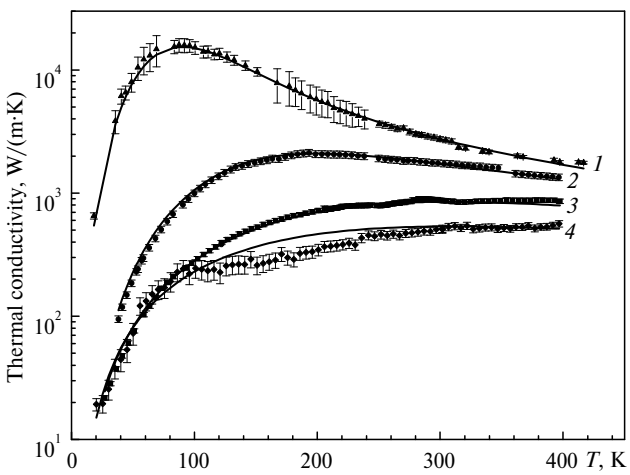

Fig. 7. Measured and calculated thermal conductivity of diamond samples with different boron content; experimental results: ▲ – II*a* (from [9]); ● – $5 \cdot 10^{18}$ cm^{-3} (from [9]); ■ – $2 \cdot 10^{19}$ cm^{-3}; ♦ – $5 \cdot 10^{19}$ cm^{-3}; theoretical calculation: *1* – II*a* (from [9]); *2* – $5 \cdot 10^{18}$ cm^{-3} (from [9]); *3* – $2 \cdot 10^{19}$ cm^{-3}; *4* – $5 \cdot 10^{19}$ cm^{-3}.

One can see that the dislocation densities in single-crystal BDDs with $2 \cdot 10^{19}$ and $5 \cdot 10^{19}$ cm^{-3} of boron are similar. It equals to ~ $7 \cdot 10^5$ cm^{-2} which is substantially less than ~ $2 \cdot 10^6$ cm^{-2} in BDD with $5 \cdot 10^{18}$ cm^{-3} boron content (see Fig. 6, *a*).

X-ray topography (see Fig. 3) indicates that apart of the boundaries of growth sectors the density of extended defects is not very high, but it is higher in more heavily boron-doped sample.

Before applying Callaway model of thermal conductivity for semiconductors one should estimate the contribution of electronic thermal conductivity. The electrical conductivity of heavily boron-doped diamond is lower than 5 Ω·cm at 300 K and drops sharply at lower temperatures. Then, according to Wiedemann-Franz law

$$k_e = 3\left(\frac{k_B}{e}\right)^2 \sigma T \approx 3 \cdot 10^{-3} \frac{W}{mK}. \qquad (1)$$

This estimation shows that electronic thermal conductivity is more than 5 orders less than measured thermal conductivity. That means that in the case of boron-doped diamond we can neglect the electronic contribution and consider only phonon thermal conductivity.

Callaway model was used to analyze experimental results in the same way it was done in [9]. The total scattering time of acoustic phonons is given by

$$\frac{1}{\tau} = \sum_i \frac{1}{\tau_i}. \tag{2}$$

Detailed description of different process of phonon scattering and expressions for their characteristic scattering time can be found in [4], [10].

For normal processes [4]

$$\frac{1}{\tau_N} = AT^3 \frac{\omega}{2\pi}. \tag{3}$$

Here A – temperature independent parameter; T – temperature; ω – phonon frequency.

For umklapp processes [10]

$$\frac{1}{\tau_U} = B\upsilon\lambda^{-2} T e^{\frac{-C\theta_D}{T}}, \tag{4}$$

B, C – temperature independent parameters; λ – phonon wavelength; υ – average sound velocity in the material.

For boundary scattering [10]

$$\frac{1}{\tau_b} = \frac{\upsilon}{d}, \tag{5}$$

d – parameter related to sample size.

Due to mass difference of host atoms and lattice deformations caused by doping, phonon scattering time for point defects [10]:

$$\frac{1}{\tau_p} = \left\{ \left[\frac{V_0}{4\pi\upsilon^3} \left(\frac{\delta M}{M} \right)^2 + \frac{2n_p V_0^2}{\pi\upsilon^3} \left(\frac{\delta R}{R} \right)^2 \right] \omega^4 \right\}^{-1}, \tag{6}$$

M – atomic mass of the crystal; δM – difference between masses of substitutional and host atoms; R, δR – radius of the host atom and difference between radiuses of substitutional and host atoms; V_0 – volume per atom; n_p – point defects density.

To take into account a phonon scattering on dislocations we need to consider two main factors: scattering on irregularities within crystal and on elastic field arose around them. In [10] the following expressions for scattering times are given:

$$\frac{1}{\tau_{core}} = K_1 N_D \frac{r^4}{\upsilon^2} \omega^3; \tag{7}$$

$$\frac{1}{\tau_{str}} = K_2 N_D \frac{\gamma^2 B_D^2}{2\pi} \omega, \tag{8}$$

K_1, K_2 – temperature independent parameters; N_D – dislocation density; B_D – Burgers vector of the dislocation; r – dislocation radius; γ – Gruneisen parameter.

In the previous work we determined parameters A, B and C in (3) and (4) for II*a* diamond and II*b* diamond with ~ $5 \cdot 10^{18}$ cm^{-3} boron content. From fitting the data on BDD with $5 \cdot 10^{18}$ cm^{-3} boron we determined parameters K_1 and K_2 in expressions (7) and (8), which describe phonon-dislocation scattering. The values of these parameters are given in the table.

Parameter of the model	Process	Value	Reference
A	Normal processes (Eq. 3)	$1.9 \cdot 10^{-11}$ K^{-3}	[9]
B	Umklapp processes (Eq. 4)	$2.2 \cdot 10^{-12}$ cm·K^{-1}	[9]
C	Umklapp processes (Eq. 4)	670 K	[9]
K_1	Dislocation core scattering (Eq. 7)	$8.8 \cdot 10^{3}$	This work
K_2	Elastic field scattering (Eq. 8)	$9.6 \cdot 10^{5}$	This work

We estimated the dislocation density of BDDs with $2 \cdot 10^{19}$ and $5 \cdot 10^{19}$ cm^{-3} of boron from the best fit with the model parameters from the table. The corresponding graphs are shown in Fig. 8.

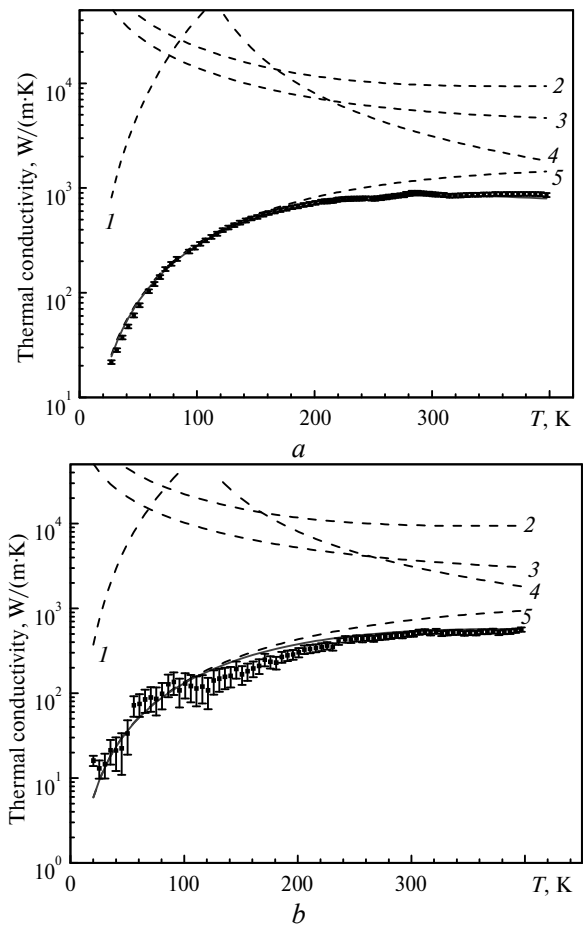

Fig. 8. Calculated impacts of different processes of phonon scattering on the total thermal conductivity of single-crystal BDD with $2 \cdot 10^{19}$ (*a*) and $5 \cdot 10^{19}$ cm^{-3} (*b*) of boron: *1* – boundery scattering; *2* – umklapp processes; *3* – boron atoms; *4* – isotopes (n(^{13}C) = 1.1 %); *5* – dislocations; *6* – total thermal conductivity; ■ – experimental results.

Each line (see Fig. 8) is the calculated thermal conductivity in a presence of only one process of phonon scattering. Thus, the total thermal conductivity is "lower than the lowest".

The best fit of experimental data was achieved at dislocation densities of $\sim 3.7 \cdot 10^6$ and $\sim 3.6 \cdot 10^7$ cm^{-2} for BDDs with $2 \cdot 10^{19}$ and $5 \cdot 10^{19}$ cm^{-3} boron content respectively. These values are more than an order of magnitude higher than the ones measured by etch pits counting (see Fig. 7).

The real dislocation density may be underestimated using etch pits pictures if screw dislocations with opposite screw orientation locate close each other and compensate its elastic strain field. In this case, they do not provide etch pits but phonons still can scatter on dislocation core.

Otherwise, if the dislocation density indeed does not increase with boron content rise and change of the crystal habitus, some other defects must cause thermal conductivity drop. That can be B–C and B–B pairs or some more complicated defects. In [14] Polyakov et al. suggest the formation of B–C pairs which further evaluate into plain B–C clusters called nanosheets. Such defects may have greater scattering cross-section than single substitutional boron atom and therefore affect the thermal conductivity stronger. Some fundamental conversion may take place in BDD lattice defects structure with an increase of boron content above $\sim 5 \cdot 10^{18}$ cm^{-3} and change of the grown crystal habitus. The thermal conductivity of such BDDs may be explained within Callaway model framework if new types of defects with other scattering times take part in phonon-defect scattering.

CONCLUSIONS

We have grown single crystal boron-doped diamonds with boron content of $\sim 2 \cdot 10^{19}$ and $\sim 5 \cdot 10^{19}$ cm^{-3} and investigated their thermal conductivity in the temperature range of 20–400 K. Generally, the thermal conductivity decreases with boron content increase. We analyzed the obtained data within Callaway model framework. Fitting the experimental data with theoretical curves gave the densities of extended defects much higher than the values obtained by etch pits counting. The densities of etch pits in more heavily boron-doped crystals is less than in the crystal with $5 \cdot 10^{18}$ cm^{-3} boron content. We suppose that either neighbor screw dislocation of the opposite sign effectively reduce lattice tensions, thus the density of etch pits reduces, or a new type of extended defects with the unknown phonon scattering time appear. The change of the grown crystal habitus from cubooctahedral to octahedral one at boron content above $5 \cdot 10^{18}$ cm^{-3} may also be associated with a change in the structure of lattice defects. The temperature dependence of thermal conductivity of such BDDs may be described within Callaway model framework if new types of defects with other scattering times take part in phonon-defect scattering or if the density of etch pits is really substantially less than the real density of extended defects.

ACKNOWLEDGEMENTS

This work was carried out using the facility of the Shared-Use Equipment Center of the Technological Institute for Superhard and Novel Carbon Materials supported by Ministry of Education and Science of Russian Federation within the agreement RFMEFI59317X0007 #14.593.21.007

Теплопровідність монокристала, легованого бору (BDD) із вмістом бору $\sim 2 \cdot 10^{19}$ *см*$^{-3}$ *(~ 120 ppm) та* $5 \cdot 10^{19}$ *см*$^{-3}$ *(~ 300 ppm), було вивчено прийнятим методом в температурному діапазоні 20–400 К. Результати було проаналізовано в рамках моделі*

Каллавэй. Отримані значення щільності дислокацій добре узгоджуються з експериментальними даними і збігаються зі щільністю яскравих ямок травлення. Їх відмінність передбачає наявність деяких інших пов'язаних з бором дефектів в кристалічній решітці.

***Ключові слова**: алмаз, легований бором, теплопровідність, високий тиск, висока температура, плотність дислокацій.*

Теплопроводность монокристалла, легированного бором (BDD) с содержанием бора ~ $2 \cdot 10^{19}$ $см^{-3}$ (~ 120 ppm) и $5 \cdot 10^{19}$ $см^{-3}$ (~ 300 ppm), была изучена принятым методом в температурном диапазоне 20–400 K. Полученные данные были проанализированы в рамках модели Каллавэй. Полученные значения плотности дислокаций хорошо согласовывались с экспериментальными данными и сравнивались с плотностью ямок травления. Их различие предполагает присутствие некоторых других связанных с бором дефектов в кристаллической решетке.

***Ключевые слова**: алмаз, легированный бором, теплопроводность, высокое давление, высокая температура, плотность дислокаций.*

1. Onn D., Witek A., Qiu Y., Anthony T., Banholzer W. Some aspects of the thermal conductivity of isotopically enriched diamond single crystals. *Phys. Rev. Lett.* 1992. Vol. 68, no. 18. P. 2806–2809.
2. Olson J., Pohl R., Vandersande J., Zoltan A., Anthony T., Banholzer W. Thermal conductivity of diamond between 170 and 1200 K and the isotope effect *Phys. Rev. B*. 1993. Vol. 47, no. 22. P. 14850–14856.
3. Anthony T.R., Banholzer W.F., Fleischer J.F., Wei Lanhua, Kuo P.K., Thomas R.L., Pryor R.W. Thermal diffusivity of isotopically enriched C12 diamond. *Phys. Rev. B*. 1990. Vol. 42, no. 2. P. 1104–1111.
4. Wei L., Kuo P.K., Thomas R.L., Anthony T.R., Banholzer W.F. Thermal conductivity of isotopically modified single crystal diamond. *Phys. Rev. Lett.* 1993. Vol. 70, no. 24. P. 3764–3767.
5. Callaway J. Model for lattice thermal conductivity at low temperatures, *Phys. Rev.* 1959. Vol. 113, no. 4. P. 1046–1051.
6. Bormashov V.S., Buga S.G., Blank V.D., Kuznetsov M.S., Nosukhin S.A., Terent'ev S.A., Pel' E.G. Fast-response thermistors made of synthetic single-crystal diamonds. *Instrum. Exper. Techn*. 2009. Vol. 52, no. 5. P. 738–742.
7. Blank V.D., Bormashov V.S., Tarelkin S.A., Buga S.G., Kuznetsov M.S., Teteruk D.V., Kornilov N.V., Terentiev S.A., Volkov A.P. Power high-voltage and fast response Schottky barrier diamond diodes. *Diamond Relat. Mater*. 2015. Vol. 57. P. 32–36.
8. Tarelkin S. Bormashov V., Buga S., Volkov A., Teteruk D., Kornilov N., Kuznetsov M., Terentiev S., Golovanov A., Blank V. Power diamond vertical Schottky barrier diode with 10 A forward current. *Phys. Status Solidi A*. 2015. Vol. 212, no. 11. P. 2621.
9. Prikhodko D., Tarelkin S., Bormashov V., Golovanov A., Kuznetsov M., Teteruk D., Volkov A., Buga S. Thermal conductivity of synthetic boron-doped single-crystal HPHT diamond from 20 to 400 K. *MRS Commun*. 2016. Mar. P. 1–6.
10. Thermal conductivity: theory, properties, and applications. Ed. T.M. Tritt. New York: Kluwer Academic/Plenum Publishers, 2004.
11. Bormashov V.S., Tarelkin S. A., Buga S.G., Kuznetsov M.S., Terentiev S.A., Semenov A.N., Blank V.D. Electrical properties of the high quality boron-doped synthetic single-crystal diamonds grown by the temperature gradient method. *Diamond Relat. Mater*. 2013. Vol. 35. P. 19–23.
12. Blank V.D., Kuznetsov M.S., Nosukhin S.A., Terentiev S.A., Denisov V.N. The influence of crystallization temperature and boron concentration in growth environment on its distribution in growth sectors of type II*b* diamond, *Diamond Relat. Mater.* 2007. Vol. 16, no. 4–7. P. 800–804.
13. Tarelkin S.A., Bormashov V.S., Kuznetsov M. S., Buga S.G., Terentiev S.A., Prikhodko D.D., Golovanov A.V., Blank V.D. Heat capacity of bulk boron doped single crystal HPHT diamonds in the temperature range from 2 K to 400 K. *J. Superhard Mater*. 2016. Vol. 38, no. 6. P. 412–416.
14. Polyakov S.N., Denisov V.N., Mavrin B.N., Kirichenko A.N., Kuznetsov M.S., Martyushov S.Yu., Terentiev S.A., Blank V.D. Formation of boron-carbon nanosheets and bilayers in boron-doped diamond: origin of metallicity and superconductivity. *Nanoscale Res. Lett*. 2016. Vol. 11, no. 1. P. 1–9.

Received 28.11.17
Revised 07.02.18
Accepted 12.02.18